Chaotic Modeling and Simulation (CMSIM) **1: 99-112, 2016**

Predicting and Simulating Chaotic Instabilities in an Inclined Furuta Pendulum

Paul A. Meehan[1]

[1] School of Engineering, University of Queensland, Brisbane, Qld. 4072. Australia
(E-mail: meehan@uq.edu.au)

Abstract. The occurrence of chaotic instabilities is investigated in the swing motion of an inclined Furuta pendulum. The analysis is motivated and applied to predicting the nonlinear bucket swing behaviour of a dragline. A dragline is a large, powerful, inclined Furuta pendulum utilized in the mining industry for removal of overburden. A representative model of the dynamical system with energy dissipation is first developed and pertinent equilibrium states are identified and unperturbed phase space behaviour determined. Fundamental insights into the effects of inclination angle on the equilibrium behaviour are identified. Subsequently, analytical predictive criteria for the onset of chaotic instability in the forced system are obtained in terms of critical system parameters using Melnikov's method. Numerical simulations under field measured conditions are performed and show that the sufficient analytical criteria are useful predictors of the onset of chaotic instability under steady and unsteady slewing conditions. Results for both inclined (tight dragrope) and non-inclined (loose dragrope) conditions are compared and discussed. The inclination is shown to critically change the equilibrium behaviour of the system and delay the onset of chaotic instability primarily due to centrifugal stiffening of the pendulum swing. In addition, conditions under which chaotic instability is more likely to occur such as pendulum mass/bucket positions are identified and discussed.

Keywords: chaotic motion, Furuta pendulum, dragline, Melnikov's method.

1 Introduction

The analysis of the nonlinear dynamics of a pendulum on a rotating arm (Furuta pendulum) has been the topic of much recent research. The system is a fundamental rotating multibody system that may be used to provide insight into the dynamic behaviour of a wide range of more complex systems including satellites and mining draglines (see for examples Moon[i], Kapitaniak[ii], Fradkov and Evans [iii], Meehan et al [iv,v,vi], Holmes and Marsden[vii] and Koiller[viii] amongst many others). The Furuta pendulum is also a classic nonlinear benchmark system for proving and tuning nonlinear control strategies [ix,x,xi]. Recent research on this system has identified interesting nonlinear and stability behaviour of the non-inclined Furuta pendulum. In particular, Pagano et al[xii] identified pitchfork and Hopf bifurcations using centre manifold and

Revised received: 14 January 2016 / Accepted: 27 January 2016

ISSN 2241-0503

normal form theories providing insight into control parameter tuning for upright position stabilization. This bifurcation analysis was extended recently in Munoz et al[x] to identify new branching point bifurcations. These researchers noted possibilities of further contributions, facilitated by insight from investigations on analogous pendulum systems. In fact, in parallel, this research was extended using analogous methodology from a fundamental rotating multibody system in the form of a very large practical Furuta pendulum; a dragline[vi]. Draglines are crane-like machines used as the primary means for removal of overburden in open-cut coal mining. The nonlinear dynamics of the dragline bucket (pendulum mass) swing motion during house (rotating arm) slewing (rotation) is of importance[xiii], as excessive amplitudes cause fatigue damage and render the system difficult to control. The recent research on this system specifically extended the work of Munoz et al[x] in that an analytical closed form Melnikov solution for prediction of the onset of chaotic instability in the non-inclined Furuta pendulum was obtained and validated using numerical simulations under small and large perturbative slew torque conditions. Although these analytical results are extremely useful for avoiding and or controlling chaos in the non-inclined Furuta pendulum, the scope of application to dragline behaviour is limited in that the dragrope must be assumed to be slack. In fact, the dragrope is often taught at times during a normal cycle of operation, causing the pendulum bucket to swing in a plane inclined to the vertical as opposed to being parallel to the axis of the rotating arm (slew axis, see fig 1). Hence a dragline with a taut drag rope is an example of a large inclined Furuta pendulum. The effects of such an inclination on the dynamic behaviour of the Furuta pendulum are unknown and are shown to be non-intuitive in the present research. Hence, the main contributions of this paper are:

- Analytical determination of the equilibrium and stability behaviour of the inclined Furuta pendulum identifying fundamental differences with the non-inclined system.
- Analytical prediction of the occurrence of chaotic instability of the inclined Furuta pendulum.
- Application and validation of analytical predictions using simulations based on field measured parameters and data and comparisons with the non-inclined system.

In this paper, a formulation of the nonlinear equations of motion governing the dynamics of the inclined Furuta pendulum/dragline system are first presented. Unperturbed phase space analysis results are then described and equilibria and nonlinear behavior are identified. Numerical and analytical results, describing the presence of chaotic instabilities under different operating conditions, are compared under quasistatic conditions before a full analysis using field data of a dragline cycle is provided. Conditions under which chaotic instability is more likely to occur, including regions in pendulum mass/bucket trajectory space, are identified and discussed.

2 Modelling the Inclined Furuta Pendulum

A dragline system is an analog of an inclined Furuta pendulum as shown via comparison in Figure 1. The system consists of a rotating assembly comprised of a house (containing primary components such as drive motors, controls and an operator cabin), a boom structure and a bucket, as shown in the model of Fig. 1a). The normal dragline operation cycle consists of three main phases: 1) a digging phase, in which the bucket is filled with overburden; 2) a slew phase, in which the house and boom is swung (or slewed) about a vertical axis while the bucket is hoisted, and 3) a dump and return slew phase during which the overburden is dumped and the house and boom return to the dig position. Control of the hoist and drag rope lengths allows positioning of the bucket in the vertical boom plane. However, the bucket is free to swing normal to that plane and a considerable amount of operator skill is required to control this undesirable motion.

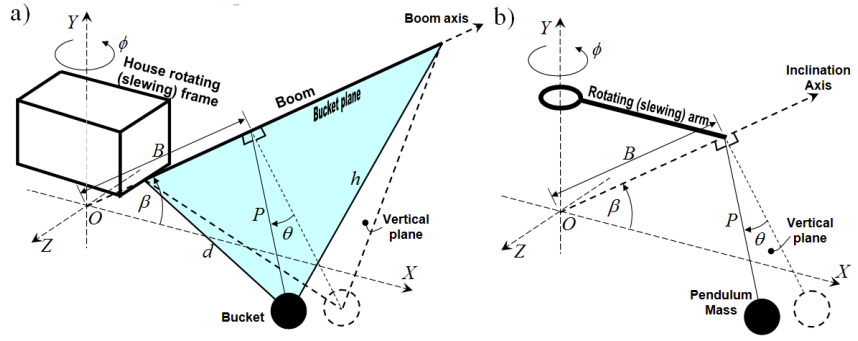

Fig. 1. Equivalent models of an inclined Furuta pendulum; a) slewing dragline with tight dragrope, b) generic model.

For the purposes of investigating nonlinear behaviour of the dragline, an inclined Furuta pendulum model based on Fig. 1 is developed. Referring to Fig. 1, the house and boom structure (rotating arm) is modelled as a rigid body with moment of inertia, I_h, that slews about the vertical slew rotation axis Y. The boom is inclined at an angle β with respect to the horizontal X axis of the inertial reference frame XYZ with the origin O at the intersection of the boom axis and the vertical. The bucket/pendulum mass is modelled as a point mass, m, suspended by the massless drag and hoist ropes of lengths, d and h, which control the motion of the bucket within the bucket plane. The bucket position is defined by the four independent degrees of freedom: ϕ, θ, P and B. The slew angle, ϕ, is a measure of the rotation of the rigid house and boom assembly about the Y axis. The out of plane angle, θ, represents the angle between the vertical plane through the boom axis and the bucket plane. It is noted that the tight dragrope enforces the bucket to swing about the boom axis as opposed to a horizontal axis with a loose drag rope ie the system becomes an inclined Furuta pendulum as opposed to non-inclined. In this case, the location

of the bucket within the bucket plane is measured along two orthogonal axes, B parallel to the boom axis and P perpendicular to this axis. The bucket is considered to be acted upon by gravity, *g*, in the *–Y* direction, and has a damping torque proportional to the bucket out-of-plane angular velocity. This damping torque is associated with viscous losses in the ropes and sheaves and has a constant, c_t. A net slew torque, *M*, about the *Y*-axis is generated from the slew transmission controlled by the operator.

The equations of motion for the system for the two rotational degrees of freedom, ϕ and θ, may be derived using Lagrange's Equations in a similar manner to [vi] as,

$$\ddot{\phi}\underset{\sim}{I} + m\left(\ddot{\theta}P\underset{\sim}{D}_2 - \dot{\theta}^2 PB\sin\theta\cos\beta + 2\dot{\phi}\dot{\theta}P\sin\theta\left(P\cos\theta - \underset{\sim}{D}_1\sin\beta\right)\right) = M \quad (1)$$

$$m\left(\ddot{\theta}P^2 + gP\cos\beta\sin\theta + \ddot{\phi}P\underset{\sim}{D}_2 - \dot{\phi}^2 P\sin\theta\left(P\cos\theta - \underset{\sim}{D}_1\sin\beta\right)\right) + c_t\dot{\theta} = 0 \,, \quad (2)$$

where the underscore $\sim$ indicates functions of the degrees of freedom as defined in the Appendix as follows; $\underset{\sim}{D}_1$ is the horizontal distance from the slew axis to bucket image in the vertical boom plane, $\underset{\sim}{D}_2$ is the perpendicular horizontal distance from the bucket swing velocity to the slew axis and $\underset{\sim}{I}$ represents the instantaneous moment of inertia of the system about the Y axis.

In the context of a dragline model, these inclined Furuta pendulum equations are simplified in that the bucket position coordinates, *P* and *B*, are considered to be quasistatically constant. Equation (1) can be considered to be the slew moment equation about the *Y* axis. The first term arises from the slew acceleration with the instantaneous system moment of inertia $\underset{\sim}{I}$ determined by the bucket position in the horizontal plane as a function of swing angle θ as well as *P* and *B*. The last three terms represent the additional moments contributed from the bucket swing motion via Coriolis and other inertia forces with respect to O. Equation (2) represents the moment equation for the bucket swing motion about the boom axis. The first two terms and the last are typical for a damped pendulum, while the other two terms characterise the effects of the centrifugal and angular accelerations contributions from the slew motion, arising due to the moving reference plane. Equations (1) and (2) are coupled through multiple non-linear terms resulting from the rotating multibody motion of the system.

At this point it is instructive to understand how the inclination angle of the inclined Furuta system (due to a tight dragrope) has affected the equations of motion, as compared to the non-inclined system (see [vi]). Firstly, gravity will now act at an angle β with respect to the pendulum-bucket swing motion and hence the natural frequency of the bucket swing under no slewing $\dot{\phi} = 0$ reduces to $\omega_o = \sqrt{\mathrm{g}\cos\beta/P}$. Secondly, the bucket swing motion is no longer in a plane parallel to the slew axis. This means that there will now be a component of centrifugal force due to slewing in the plane of the bucket swing motion. This component is evident in the fourth terms of (1) and (2) as the factor $-\underset{\sim}{D}_1\sin\beta$ and will cause a centrifugal stiffening of the bucket swing behaviour. This is

shown to critically affect the stability and perturbed nonlinear behaviour of the system in the subsequent sections.

For subsequent analysis, it is convenient to define the energy and angular momentum quantities that are conserved under unperturbed conditions. The total mechanical energy of the system, *E*, is derived as,

$$E = \tfrac{1}{2}\underset{\sim}{I}\dot{\phi}^2 + \tfrac{1}{2}mP^2\dot{\theta}^2 + m\underset{\sim}{D}_2 P\dot{\phi}\dot{\theta} + mgP\cos\beta(1-\cos\theta), \qquad (3)$$

where presently for simplicity the potential energy is defined as being zero when the bucket swing angle $\theta = \theta^{l}$. Similarly, the Y component of angular momentum of the system about O, $H_{Oy,}$ that is conserved when $M = 0$, may also be obtained as,

$$H_{Oy} = \underset{\sim}{I}\dot{\phi} + mP\dot{\theta}\underset{\sim}{D}_2, \quad . \qquad (4)$$

3 Phase Space Analysis of the Inclined Furuta Pendulum

The phase space of the unperturbed system, corresponding to the case of no external torque $M = 0$ and no damping $c_t = 0$, was investigated for stability and nonlinear behaviour. For the unperturbed system, both angular momentum and total energy of the system have constant values $\mathrm{H_{Oy}}$ and E, such that by using Eqs. (3) and (4), the phase space may be described by,

$$\dot{\theta}^2 = \frac{2\underset{\sim}{I}\left(\mathrm{E} - mgP\cos\beta(1-\cos\theta)\right) - \mathrm{H_{Oy}}^2}{mP^2(I_h + m(P^2+B^2)\cos^2\beta\sin^2\theta)}. \qquad (5)$$

Equation (5) is in a similar (but distinct) form to that of the previous analyses (eg [vi]) for the non-inverted Furuta pendulum and may also be shown to be integrable; a necessary condition for application of Melnikov's method. The corresponding set of phase curves under different energy and angular momentum conditions for different values of $\mathrm{C} = 2\mathrm{E}I - \mathrm{H_{Oy}}^2$ are plotted in Fig. 2. These phase space plots are representative of the unperturbed dynamics of the inclined Furuta pendulum for out of plane bucket angles of magnitude less than π [2]. Fig. 2a) corresponds to the two equilibrium conditions described by

$$\left[\theta \quad \dot{\phi}\right]^{\mathrm{T}} = \left[\pm\theta^{*} \quad \sqrt{g\cos\beta/(P\cos\theta^{*} - \underset{\sim}{D}_1^{*}\sin\beta)}\right]^{\mathrm{T}}, \text{ if } \mathrm{H_{Oy}}^2 > \left(I\dot{\phi}_{crit}\right)^2 \quad (6)$$

---

[1] Note in the derivation in the Appendix the potential energy reference is defined more generally to (3) as the origin O.

[2] For larger, out of plane bucket angles, the phase space has heteroclinic orbits intersecting at the inverted unstable equilibrium points defined by $\theta = \pm n\pi$, similar to the phase space of a simple pendulum [7-10]. These represent unrealistic conditions for a dragline so are not investigated further in the present analysis.

while Fig. 2b) corresponds to that described by

$$\left[\theta \quad \dot{\phi}\right]^{\mathrm{T}} = \left[0 \quad \mathrm{H_{Oy}}/I\right]^{\mathrm{T}}, \text{. if } \mathrm{H_{Oy}}^2 \le \left(I\dot{\phi}_{crit}\right)^2 \tag{7}$$

where θ^* is a function of the parameters, $\mathrm{H_{Oy}}$ and I, as defined by the roots of a fourth order polynomial,

$$\theta^* = \cos^{-1}\left[root\left(\left(I_h + m[P^2 + B^2 - (B\sin\beta - xP\cos\beta)^2]\right)^2 + \mathrm{H_{Oy}}^2 (B\sin\beta - xP\cos\beta)/g = 0\right)\right] \tag{8}$$

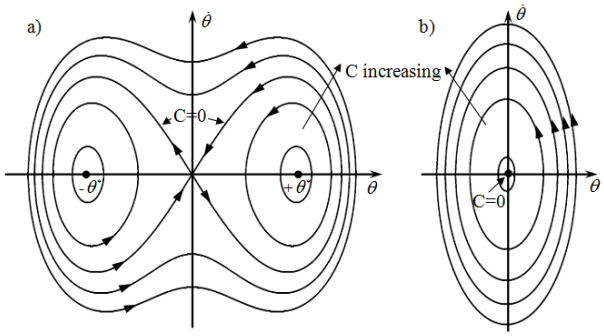

Fig. 2. Phase space curves for an inclined Furuta pendulum without external forcing or dissipation; a) $\mathrm{H_{Oy}}^2 > \left(I\dot{\phi}_{crit}\right)^2$, b) $\mathrm{H_{Oy}}^2 \le \left(I\dot{\phi}_{crit}\right)^2$. .

The stability of these equilibrium points may be derived using Lyapunov's direct method. Physically, the symmetrical properties of the bucket swing allow the possibility of two stable equilibrium points, corresponding to positive and negative swing displacements of the bucket/pendulum mass, $\pm\theta^*$. This pair of offset stable equilibrium points (also occurring in a variety of analogous systems eg [iv]) are interesting physically in that they serve to limit the slew rate to a constant critical value,

$$\dot{\phi}_{crit} = \sqrt{g/h_Y}, \quad h_Y = P\cos\beta - B\sin\beta. \tag{9}$$

where h_Y is the vertical distance of the bucket below the X axis when the bucket swing angle is zero. In contrast to the non-inclined Furuta pendulum, it is deduced that the inclination critically changes the stability behaviour, delaying the existence of the two stable equilibrium points to conditions when the bucket is below the horizontal (ie longer rope lengths) and to a higher critical slew rate, $\dot{\phi}_{crit} = \sqrt{g/h_Y} \ge \sqrt{g/P}$. The existence of a pair of homoclinic orbits in Fig. 2a) encircling the two equilibrium points is important as the system will be attracted to either one of the equilibrium points depending on the initial conditions and there will be a region in phase space where this dependence will be highly sensitive to small changes. By solving for the origin point using Eq.(5), the set of homoclinic orbits is found to occur under the conditions,

$$\mathrm{C} = 2\mathrm{E}I - \mathrm{H_{Oy}}^2 = 0 \quad \text{and} \quad \{\mathrm{H_{Oy}}^2 > I^2 g/h_Y \quad \text{where} \quad h_Y < 0\}. \tag{10}$$

It may be deduced that the pitchfork bifurcation to the homoclinic orbits in Fig. 2a) occurs when the angular momentum first exceeds the critical value described by eqn (6). With reference to chaotic instability, it is therefore expected that it's onset will first occur for small bucket swing angles once the slew velocity exceeds $\sqrt{g/h_Y}$. This is investigated subsequently.

4 Analytical Prediction Of Chaotic Instability

The stability and phase space analyses have shown that the inclination of the Furuta pendulum significantly delays the pitchfork bifurcation (to a pair of homoclinic orbits) to a higher critical slew rate $\sqrt{g/h_Y}$. However, qualitatively the inclined system in phase space appears to behave in a similar manner to the non-inclined case when the two stable equilibrium points exist. This insight motivated an investigation into appropriate transformations of system equations in order to take advantage of the existing Melnikov analysis for the non-inclined case[vi]. For this purpose, nontrivial transformations of the energy and angular momentum quantities were investigated to non-dimensionalise the representative Lagrangian L=T-V to analogous forms. In particular, under the assumption of a small bucket swing angle, the harmonic terms of (1) and (2) are approximated by,

$$\sin\theta \approx \theta\,,\ 1-\cos\theta \approx \theta^2/2, \tag{11}$$

and the system dynamics reduce to a Lagrangian form of a rotating body with internal energy dissipation[v], described by,

$$\hat{L} = \left[\hat{\mathrm{H}}_{\mathrm{Oy}}{}^2 + (\hat{I}-1+y^2)y'^2\right] \Big/ (\hat{I}+y^2) - \hat{k}\hat{y}^2/2\,. \tag{12}$$

In (12) the dimensionless quantities are defined for the inclined Furuta pendulum as,

$$\tau = \Omega t\,,\ \hat{y} = \frac{\theta}{\hat{d}}\,,\ \hat{d}^2 = \frac{I}{mP\cos\beta h_Y} - \frac{I_h}{m\cos^2\beta(D^2+h_Y{}^2)}\,,\ \hat{I} = \frac{I}{mP\cos\beta h_Y \hat{d}^2}\,,$$

$$\hat{\mathrm{k}} = \frac{\dot{\phi}_{crit}{}^2}{\Omega^2\left[1+(D/h_Y)^2\right]}\,,\ \hat{\mathrm{H}}_{Oy} = \frac{\mathrm{H}_{Oy}}{mP\cos\beta h_Y \hat{d}^2\Omega\sqrt{1+(D/h_Y)^2}}\,,$$

$$\left\{\hat{L},\hat{E}\right\} = \frac{\{L,E\}}{mP\cos\beta h_Y \hat{d}^2\Omega^2\left[1+(D/h_Y)^2\right]}\,. \tag{13}$$

The forcing/perturbative parameters for Hamiltonian transformation may be nondimensionalised to,

$$\hat{M} = \frac{M}{mP\cos\beta h_Y \hat{d}^2\Omega^2\left[1+(D/h_Y)^2\right]}\,,\ \hat{\mathrm{c}} = \frac{\mathrm{c_t}}{mP\cos\beta h_Y \Omega\left[1+(D/h_Y)^2\right]}\,, \tag{14}$$

where the static radial distance of the bucket from the slew axis is defined as,

$$D = \underset{\sim}{D}_1(\theta=0) = \underset{\sim}{D}_2(\theta=0) = B\cos\beta + P\sin\beta\,. \tag{15}$$

Although this nondimensional parameterisation was onerous and may seem convoluted, the transformed Lagrangian (12) is now identical to that of the non-inclined system and hence the resulting Hamiltonian equations of motion, their homoclinic orbit solutions and Melnikov analyses can now be conveniently applied to the present problem. For brevity, the primary steps of the Melnikov analysis are outlined in the following, as details of a very similar analysis is provided in [iv].

Prediction under Perturbed Steady Slewing Conditions

Melnikov's method was used to obtain an analytical criterion for the onset of chaotic instability in the perturbed dragline system based upon the unperturbed phase space. The simplest form of Melnikov's method considers systems of the form:

$$\dot{\mathbf{x}} = \mathbf{f}(\mathbf{x}) + \varepsilon \mathbf{g}(\mathbf{x}, t); \quad \mathbf{x} = \begin{pmatrix} u & v \end{pmatrix}^T \in \Re^2 \qquad (16)$$

where $\mathbf{f}(\mathbf{x})$ is considered to be the unperturbed Hamiltonian system of state equations defined on $\Re^2$, and $\varepsilon \mathbf{g}(\mathbf{x}, t)$ is a small periodic perturbation which is not necessarily Hamiltonian. Using the dimensionless quantities of (13) and (14), the equations of motion for the inclined Furuta pendulum (1) and (2) can be expressed in the Hamiltonian form of (16) as,

$$\begin{aligned} d\hat{y}/d\tau_\Omega &= \hat{p}_y \left(\hat{\mathrm{I}} + \hat{y}^2\right)\left(\hat{\mathrm{I}} - 1 + \hat{y}^2\right)^{-1} \\ d\hat{p}_y/d\tau_\Omega &= \frac{\hat{y}}{\left(\hat{\mathrm{I}} + \hat{y}^2\right)^2}\left\{\hat{\mathrm{H}}_{Oy}{}^2 - \hat{\mathrm{k}}\left(\hat{\mathrm{I}} + \hat{y}^2\right)^2 + \left[\hat{p}_y \left(\hat{\mathrm{I}} + \hat{y}^2\right)\beta(\hat{y})\right]^2\right\} \\ &\quad + \varepsilon\left[\hat{\mathrm{M}}_{\mathrm{E}} \cos\tau + 2\hat{y}\hat{\mathrm{M}}_{\mathrm{E}}\left(\hat{\mathrm{H}}_{Oy}/\hat{\mathrm{I}}\right)\sin\tau + \hat{y}\left(\hat{\mathrm{M}}_{\mathrm{E}}{}^2/\hat{\mathrm{I}}\right)\sin^2\tau - \hat{\mathrm{c}}\hat{p}_y\left(\hat{\mathrm{I}} + \hat{y}^2\right)^2\beta(\hat{y})\right] + O\left(\varepsilon^2\right) \end{aligned} \qquad (17)$$

where the generalised momentum, $\hat{p}_y$, is defined by,

$$\hat{p}_y = \hat{y}'\left(\hat{\mathrm{I}} - 1 + \hat{y}^2\right)\Big/\left(\hat{\mathrm{I}} + \hat{y}^2\right), \qquad (18)$$

and an external slew torque of the form $\hat{M} = \hat{\mathrm{M}}_{\mathrm{E}} \cos\tau$ is considered. For Eq. (17), a Taylor's series has been used to expand the perturbational terms with $\varepsilon = 1/\hat{\mathrm{I}}$, so that only first order terms have been retained. More details of this transformation are provided in [v]. It is noted that the unperturbed phase space $\{\hat{y}, \hat{p}_y\}$, has the same qualitative behavior as the phase space $\{\theta, \theta'\}$, illustrated in Fig. 2. Equation (17) is in the form appropriate for the application of Melnikov's method. The Melnikov function, denoted $M(\mathrm{t}_0)$ is written as the integral,

$$M(\mathrm{t}_0) = \int_{-\infty}^{\infty} \mathbf{f}\left(\mathbf{q}_0(t)\right) \wedge \mathbf{g}\left(\mathbf{q}_0(t), t + t_0\right) dt, \quad (19)$$

where $\mathbf{f}(\mathbf{x})$ and $\mathbf{g}(\mathbf{x}, t)$ have been defined previously in Eq. (16), the symbol $\wedge$ is the wedge product defined by $a \wedge b = a_1 b_2 - a_2 b_1$, and $\mathbf{q}_0(t)$ is the

solution for the set of homoclinic orbits in the unperturbed system. The equations describing the homoclinic orbits depicted in Fig. 2a), for small out of plane angle, θ, may be obtained via solution to equations (5), subject to (10), (11) and (14), as,

$$\left[\hat{y}_0 \quad d\hat{y}_0/d\tau_\Omega\right]=\left[\sqrt{\eta}\ \mathrm{sech}\left(\vartheta\tau_\Omega\right) \ - \vartheta\sqrt{\eta}\mathrm{sech}\left(\vartheta\tau_\Omega\right)\tanh\left(\vartheta\tau_\Omega\right)\right], \qquad (20)$$

where

$$\eta = 2\hat{E}/\hat{k}-\hat{I}, \quad \vartheta=\sqrt{\left(2\hat{E}-\hat{I}\hat{k}\right)/\left(\hat{I}-1\right)}, \qquad (21)$$

and the subscript $(\ )_0$ denotes the closed solution for the homoclinic orbits. Using Eqs. (20), (16) and (17) the Melnikov function may be obtained explicitly. In particular, under the assumption that $\hat{M}_E << \hat{I}\sqrt{\hat{k}/\left(\hat{I}-1\right)}$ or $\hat{M}_E << 2\hat{H}_{Oy}\cosh\left(\pi/2\vartheta\right)$, a relationship for the critical torque amplitude may be simplified to the form,

$$\hat{M}_E > \ 2\hat{c}\vartheta^3\left(5\hat{I}+2\eta\right)\Bigg/\left(15\pi\sqrt{\frac{\vartheta^2}{\eta}\mathrm{sech}^2\left(\frac{\pi}{2\vartheta}\right)+\frac{\hat{H}_{Oy}{}^2}{\hat{I}^2}\ \mathrm{cosech}^2\left(\frac{\pi}{2\vartheta}\right)}\right). \qquad (22)$$

Equation (22) represents a sufficient criterion for the occurrence of chaotic instability in an inclined Furuta pendulum under slew torque perturbations, for small bucket swing angles. It is based on perturbations about a nominal (unperturbed) condition of constant (or quasistatic) angular momentum.

5 Case Study Results

Predictions of the occurrence of chaotic instability in an inclined (tight dragrope) and non-inclined (loose dragrope) Furuta pendulum under both steady and unsteady slewing motion were investigated both analytically and numerically for realistic dragline parameters. The mechanical parameters for a standard 1370 BE dragline were used to compare with previous research results: m = 66 000 kg, c_t = 4.1 MNms, I_h = 1.588x10^9 kgm^2 and Ω =0.05 $\rightarrow$0.2 rad/s. Two different bucket positions and inclinations were investigated as shown in figure 3. Case 1a) represents the non-inclined case and is included so that direct comparison with previous results[vi] can be made. The inclined cases 1b) and 2 represent typical quasistatic bucket positions encountered during normal operation with a taut dragrope. For these parameters, the critical slew rate at which a pitchfork bifurcation first occurs under inclined and non-inclined conditions is described in table 1. The slew torque frequency was chosen to be of the same order as the actual swing cycle used in dragline operation. Numerical integration of Eqs. (1) and (2) was performed using a fourth order Runge-Kutta method with at least 200 timesteps over the bucket response cycle; ensuring convergence of the numerical solution. Plots were generated after a

number of pre-iterates (no recording) of forcing periods, in order to ensure transients had subsided.

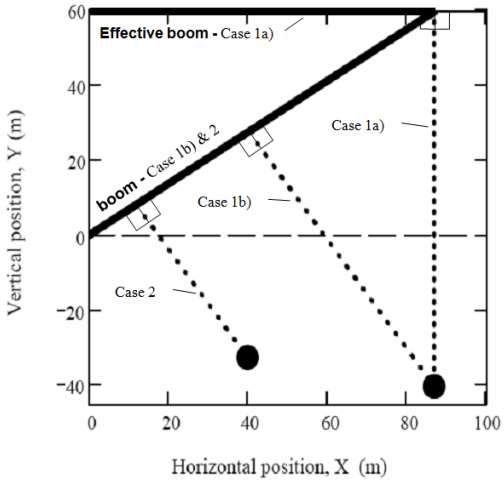

Fig. 3. Pendulum mass/bucket positions and inclinations for test cases 1a), b) & 2.

Table 1 Case configuration parameters and corresponding critical slew rates.

		β (rad)	D (m)	h_Y (m)	$\dot{\phi}_{crit}$ (rad/s)
Case 1a)	**non-inclined**	0	87	100	0.3132
Case 1b)	**inclined**	0.602	87	40.224	0.4938
Case 2	**inclined**	0.602	40	32.517	0.5492

Results under Perturbed Steady Slewing Conditions

As found with previous analyses, the occurrence of chaotic instability associated with the pitchfork bifurcation identified in section 2, is sensitive to the angular momentum of the system. In particular, according to the criterion of Eq. (22), initial slew rates only slightly greater than the critical value of $\dot{\phi}_{crit}$ were investigated to minimise the critical torque amplitude to plausible values for draglines (of order 100 MNm) and to limit bucket swing angles to realistic (small) values. In particular, unless otherwise noted, the initial slew rate was chosen to be 2% higher than the critical slew torques in Table 1. Figure 4 shows an example of a bifurcation diagram generated for the inclined Furuta case 1b) with an initial slew rate of $\dot{\phi}_i = 0.505$ rad/s, a slew torque frequency of 0.05 rad/s and 200 pre-iterates. The diagram shows evidence of steady state chaotic instability over a range of torque amplitudes, with the initial occurrence at approximately $M_E = 515$ kNm. This is notably significantly higher than that found for the non-inclined case 1a) which was $M_E = 390$ kNm [vi] for an equivalent initial slew rate factor 102% of the critical slew rate listed in Table 1.

In the same manner, the critical torque amplitudes for a number of bifurcation diagrams at different slew torque frequencies were determined in order to obtain a quantitative comparison with analytical Melnikov predictions using Eq.(22). These results were collated for the three cases of table 1 in Figure 5.

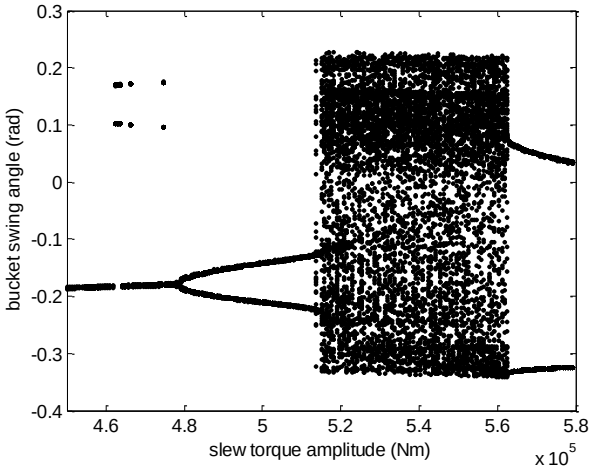

Fig. 4. Bifurcation diagram for the inclined Furuta pendulum/dragline case 1b) under perturbed, steady slew conditions ($\dot{\phi}_i = 0.505$ rad/s, $\Omega = 0.05$ rad/s)..

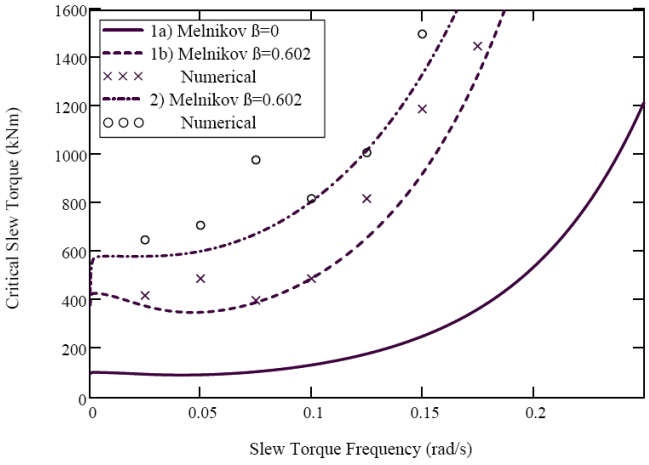

Fig. 5. Comparison of analytical and numerical results for the onset of chaotic instability for the inclined Furuta pendulum/dragline cases 1 a),b) & 2 under perturbed, steady slew conditions ($\dot{\phi}_i = 0.505$ rad/s).

Figure 5 shows good agreement between the analytical and numerical results and highlights the conservative nature of the Melnikov criterion for predicting the onset of steady-state chaotic instability in each case. By comparison between the cases of 1a) and b) it is seen that substantially higher critical torques (>3.5x) are required due to the inclination of the Furuta pendulum. This is consistent

with the occurrence of centrifugal stiffening of bucket swing motion that needs to be additionally overcome by perturbations in the inclined case. Also comparing the inclined cases 1b) and 2, it appears the relative amount of centrifugal stiffening is also associated with higher critical torques as the bucket position moves closer to the horizontal *X* axis. This is confirmed by inspection of equations (2) to reveal that the total centrifugal torque on the bucket swing motion is proportional to this distance $h_Y = (P\cos\theta - D_1 \sin\beta)/\cos\beta$. These results, under steady slewing conditions, also indicate that the dragline motion may pass through chaotic instability under larger perturbations associated with a normal (unsteady slewing) cycle of operation.

Results under Unsteady Slewing Conditions

The dragline dynamics was also investigated via numerical simulations of typical unsteady slewing conditions, with a nominal slew torque frequency of $\Omega = 0.0623$ rad/s representing a cycle time of 100 seconds. All other parameters were set values as specified previously, with exception to house slew damping, which was set to a value of c_h=8.97x10^7 Nms; obtained from field measurements. The bifurcation diagram was generated under these conditions for case 1b) and indicates the first onset of chaotic instability via bifurcations at a torque amplitude of approximately 82 MNm. This value compares favourably with the analytical prediction of 78 MNm based on exceeding the critical slew rate $\dot{\phi}_{crit}$. Trajectory simulations and the Poincare map for fully developed chaotic instability at a slightly higher torque amplitude of 84MNm are shown in Fig. 7.

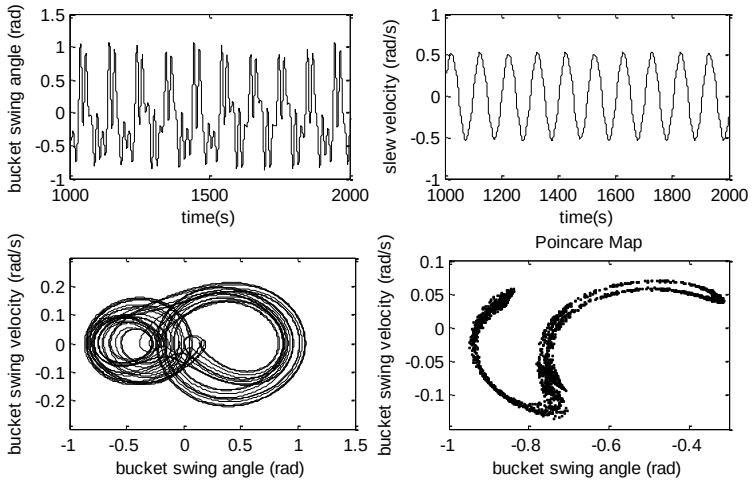

Fig. 7. Time histories and phase spaces for the inclined Furuta pendulum/dragline case 1b) under large unsteady slew conditions ($\dot{\phi}_i = 0$ rad/s, $\Omega = 0.0623$ rad/s, $M = 84 \times 10^6$ Nm).

The complexity of the time history and phase space traces and the fractal nature of the Poincare map are consistent with predictions of chaotic instability. These numerical simulations indicate that steady-state chaotic behavior persists even though the rotating arm of the inclined Furuta pendulum only has the necessary slew rate for the pitchfork homoclinic orbits to exist, for a relatively small amount of the cycle time.

6 Conclusions

Analytical and numerical results have shown the existence of chaotic instabilities in the inclined Furuta pendulum with internal energy dissipation, under perturbed steady slewing as well as unsteady conditions. In particular, a closed form analytical criteria and numerical verification of these predictions of chaotic instability are presented for this fundamental rotating multibody system. The effect of inclination is carefully investigated and is shown to critically change the equilibrium behaviour of the system causing the existence of a pitchfork bifurcation to be delayed to bucket positions below the X-axis due to centrifugal stiffening of the pendulum swing motion. An analytical criterion for the occurrence of a chaotic instability region in system parameter space has been derived using Melnikov's analysis. The chaotic region occurs near homoclinic orbits in the system's phase space associated with the pitchfork bifurcation. This is shown practically to exist in the dynamics of a slewing dragline with damping under normal operation. Subsequently the analytical results have been compared to various numerical results for different parameter configurations. It is shown that Melnikov's method provides a conservative estimate for the onset of steady state chaotic instability under steady and unsteady slewing conditions. Chaotic instability is shown to be delayed to higher torque amplitudes for inclinations of the Furuta pendulum due to centrifugal stiffening of the pendulum swing.

This analysis confirms that steady state chaotic instability is possible in dragline operating cycles, during high slew rate conditions under both tight and loose dragrope conditions. Its occurrence adversely affects dragline productivity and maintenance, and may be underlying difficulties with automation. Recommendations for useful extensions to the analysis include the investigations of the effect of dynamically changing rope lengths (rotating arm and pendulum lengths) and more realistic slew torque profiles during normal cycle operation. In particular, it is noted that cyclic rope length changes and operator slew control, intrinsic to normal dragline operation, may significantly alter the system equilibrium and stability behaviour.

ACKNOWLEDGEMENTS

The authors acknowledge the support of CRC Mining and Mr Mark Hateley and Dr Charlie McInnes for their assistance with the simulations.

References

[i] F. C. Moon, *Chaotic and Fractal Dynamics* (John Wiley & Sons, New York, 1992)
[ii] T. Kapitaniak, Chaotic Oscillations in Mechanical Systems (Manchester University Press, 1991)
[iii]A.L. Fradkov and R.J. Evans, "Control of chaos: Methods and applications in engineering." Annual Reviews in Control, 29(1), 33-56 (2005).
[iv] P. A. Meehan and S. F. Asokanthan, Chaos, Solitons and Fractals **13**, 1857-1869 (2002).
[v] P. A. Meehan and S. F. Asokanthan, International Journal of Bifurcation and Chaos **16(1)**, 1-19 (2006).
[vi] P. A. Meehan and K. J. Austin, International Journal of Nonlinear Mechanics **41(1)**, 304-312 (2006).
[vii] P. J. Holmes and J. E. Marsden, Indiana University Mathematics Journal **32(2)**, 273-309 (1983).
[viii] J. Koiller, Journal of Mathematical Physics **25(5)**, 1599-1604 (1984).
[ix] K. J. Åström and K. Furuta, "Swinging up a Pendulum by Energy Control", Automatica, 36, 278-285, 2000.
[x] F.J. Munoz-Al, "Bifurcation Behaviour of the Furuta Pendulum", International Journal of Bifurcation and Chaos, Vol. 17, No. 8, 2571–2578, 2007
[xi] C. Ibáñez, and J. Azuela, "Stabilization of the Furuta Pendulum Based on a Lyapunov Function Nonlinear Dynamics", 49(1-2), 1-8, 2007.
[xii] D. Pagano, L. Pizarro and J. Aracil, "Local Bifurcation Analysis In The Furuta Pendulum via Normal Forms", International Journal of Bifurcation and Chaos, Vol. 10, No. 5 981-995 (2000)
[xiii] P. I. Corke, G. J. Winstanley, and J. M. Roberts, IEEE International Conference on Robotics and Automation, Albuquerque, New Mexico, 1657-1662, (1997).